4, 252 (1968).
[3]R. A. Fisher, P. L. Kelley, and T. K. Gustafson, Appl. Phys. Lett. **14**, 140 (1969).
[4]A. Laubereau, Phys. Lett. **29A**, 539 (1969).
[5]H. Nakatsuka, D. Grischkowsky, and A. C. Balant, Phys. Rev. Lett. **47**, 1910 (1981).
[6]R. H. Stolen and C. Lin, Phys. Rev. A **17**, 1148 (1978).
[7]R. L. Fork, B. I. Greene, and C. V. Shank, Appl. Phys. Lett. **38**, 671 (1981).
[8]C. V. Shank, R. L. Fork, R. F. Leheny, and J. Shah, Phys. Rev. Lett. **42**, 112 (1979).
[9]A. Migus, C. V. Shank, E. P. Ippen, and R. L. Fork, Quantum. Electron. (to be published).
[10]R. L. Fork, C. V. Shank, and R. Yen (unpublished).
[11]R. H. Stolen, V. Ramaswamy, P. Kaiser, and W. Pleibel, Appl. Phys. Lett. **33**, 699 (1978).
[12]R. R. Alfano and S. L. Shapiro, Phys. Rev. Lett. **24**, 592 (1970); **24**, 585 (1970).
[13]E. B. Treacy, J. Quantum Electron. **QE-5**,454 (1969).
[14]L. F. Mollenauer, R. H. Stolen, and J. P. Gordon, Phys. Rev. Lett. **45**, 1095 (1980).

A theory of longitudinal modes in semiconductor lasers

Kam Y. Lau
Ortel Corporation, Alhambra, California 91803
Amnon Yariv
California Institute of Technology, Pasadena, California 91125

(Received 8 January 1982; accepted for publication 15 February 1982)

A theory of longitudinal mode lasing spectrum of semiconductor lasers is developed which takes into account the nonuniform carrier and photon distributions and local gain spectrum shifts inside lasers with low end mirror reflectivities. The theory gives results consistent with observed longitudinal mode behavior in lasers with reduced facet reflectivity.

PACS numbers: 42.55.Px, 42.60.Fc, 42.80.Sa

The longitudinal mode spectrum of semiconductor lasers has been studied extensively and major observed features can be understood in terms of modal competition in a common gain reservoir.[1–3] It was generally agreed that[4] gain saturation in semiconductor lasers is basically homogeneous and therefore it should oscillate in a single longitudinal mode above threshold. Time and again this was demonstrated in lasers of near-ideal structures[5–8] free from unstable transverse mode or self-pulsations, which otherwise would render the longitudinal lasing spectrum multimoded. In general, the number of lasing modes increases with increasing spontaneous emission and decreases with increasing optical power. Other subtle aspects of longitudinal mode behavior require more detailed theories, such as that including electron coherence,[9] or transverse waveguiding,[10] for satisfactory explanations.

It is well recognized that although ideal in a sense, single-mode lasers are not suitable for application in multimode fiber systems due to modal noise problems. It is important that one has a laser that is ideal in every other aspects, such as linear light-current characteristics, single transverse mode, nonpulsating output, etc., but oscillates in many longitudinal modes. It was observed that[11,12] otherwise single-mode lasers, when antireflection (AR) coated on one facet, becomes multimoded. This letter offers an explanation for this phenomenon.

A combination of several effects, all of them involving the nonuniform photon and carrier distributions in an AR coated laser, is responsible for the multimode behavior. First, the different levels of carrier densities in different parts of the laser cavity imply that the local gain spectrum varies along the length of the cavity. This shift in the gain spectrum as a function of carrier inversion density is well documented.[13] When averaged over the entire cavity, the difference in gain between neighboring longitudinal modes is reduced, which leads to an increase in the number of oscillating modes under identical optical power level. Secondly, superluminescence[14] takes effect in lasers with a low reflecting mirror ($<1\%$) which results in an effective increase in spontaneous emission contribution. Thirdly, at a certain *output* power level measured at the AR coated facet of the laser (refered to as the exit facet), the average *internal* optical power density is much lower in an AR coated laser when compared to an uncoated laser with identical *output* power. As mentioned before, and will be elucidated below, the *internal* power density determines the number of oscillating modes.

The analysis is based on the normalized forward and backward photon propagating equations in the laser cavity, written for each longitudinal mode:

$$\frac{dx_i^+}{dz} = \kappa g_i(N - N_{om})x_i^+ + \beta\kappa N, \quad (1a)$$

$$-\frac{dx_i^-}{dz} = \kappa g_i(N - N_{om})x_i^- + \beta\kappa N, \quad (1b)$$

where

$$\kappa(N - N_{om}) = G_h \Big/ \left(1 + \sum_i g_i(x_i^+ + x_i^-)\right), \quad (1c)$$

where the x^+'s and x^-'s are the forward and backward propagating photon densities (which are proportional to the light

 0003-6951/82/090763-03$01.00

intensities) for the ith mode, N is the carrier density, N_{om} is the carrier density for transparency, κ is the gain constant in cm^{-1}/(unit inversion), G_h is the unsaturated gain in cm^{-1}, β is half of the fraction of spontaneous emission entering the lasing mode, z is the distance along the active medium with $z = 0$ at the center of the laser and g_i is the gain factor for the ith mode, which is commonly approximated by a Lorentzian with its maximum at the i_0th mode.

$$g_i = 1/[1 + \alpha(i - i_0)^2] . \tag{1d}$$

The mode i_0 where the gain maximum occurs varies with carrier density and is approximately given by[13]

$$i_0 = [0.095\kappa N] + \text{an arbitrary integer} . \tag{1e}$$

Typical values are $\beta = 10^{-5}$, $\alpha = 5\times 10^{-4}$, and $\kappa N_{om} = 200$ cm^{-1}. The coupled equations (1) must be solved subjected to the boundary conditions

$$x_i^-(L/2) = R_2 x_i^+(L/2) ; \quad x_i^+(-L/2) = R_1 x_i^-(-L/2) , \tag{2}$$

where L is the length of the laser, typically 250 μm; R_1 and R_2 are the reflectivities of the end mirrors. This boundary value problem involving n coupled nonlinear differential equations does not lend itself to even easy numerical solutions. Major features can, however, be extracted with some manipulations and a minimal amount of computations.

Equations (1a) and (1b) are averaged over the entire cavity, and the forward and backward photons are summed to give the total photon density in the ith mode:

$$[A_i - B_i\kappa(\overline{N} - N_{om})]\overline{P}_i = \beta\kappa\overline{N} , \tag{3a}$$

where $P_i = x_i^+ + x_i^-$ and

$$A_i = \frac{1}{L}\frac{P_i(L/2)}{\overline{P}_i}\frac{[(R_1/R_2)^{1/2} + 1][1 - (R_1R_2)^{1/2}]}{1 + R_1} , \tag{3b}$$

$$B_i = \frac{1}{L}\int\frac{g_i(N - N_0)P_i\,dz}{[(\overline{N} - N_{om})\overline{P}_i]} , \tag{3c}$$

and $\overline{P}_i = (1/L)\int P_i\,dz =$ average photon density in the cavity, $\overline{N} = (1/L)\int N\,dz =$ average carrier density. The factor A_i involves the photon density *at* the mirror facet and is related to the rate of photon loss from the end mirrors. B_i can be regarded as the overall efficiency of stimulated emission in the cavity, which is considerably smaller than 1 because of the nonperfect overlap of the carriers and photons: the photon density is highest near the end facet where the carrier density is lowest because of local gain saturation. In the case where both mirrors are sufficiently reflective ($>20\%$), the carrier distribution is almost uniform along the length of the cavity and B_i approaches g_i. Equation (3a) can be physically interpreted as that the spontaneous emission $\kappa\beta\overline{N}$ makes up for the slightly excessive cavity loss $A_i\overline{P}_i$ over the stimulated gain $\kappa B_i(\overline{N} - N_{om})\overline{P}_i$.

The factors A_i and B_i for mode i depends on the *shape* of the photon and carrier distributions. Now, the fact is that the shape of these distributions depends strongly on the level of pumping and the mirror reflectivities, but only weakly on the mode number. This conclusion can be drawn from a direct integration of Eqs. (1a) and (1b), which gives

$$x_i^\pm = C_i^\pm \exp\left(\pm g_i\kappa\int(N - N_{om})dz\right) + \text{terms of higher orders in } \beta . \tag{4}$$

The gain factor g_i differs only slightly (parts in 10^4) from one mode to another and therefore the distributions $x_i^\pm$'s are almost identical, except for the proportionality factor C_i which determines the power in the ith mode. The small differences in the g_i's, however, plays a crucial role in determinating the C_i's when applying boundary conditions (2).

Given that the photon distribution of each mode has nearly identical shapes, one can derive the following:

$$A_i = \text{constant independent of } i , \tag{5}$$

$$\sum_i g_i[x_i^+(z) + x_i^-(z)] = S\,[x_0^+(z) + x_0^-(z)] , \tag{6}$$

where $S \approx \Sigma\overline{P}_i/\overline{P}_0$ is the ratio of the total power to that in an arbitrarily chosen 0th mode. The photon number in each mode is then computed as follows: given a value for S, the n coupled equations (1) can be reduced to two equations for the 0th mode:

$$\pm\frac{dx_0^\pm}{dz} = g_0\kappa(N - N_{om})x_0^\pm + \beta N , \tag{7}$$

$$\kappa(N - N_{om}) = G_h/[1 + S(x_0^+ + x_0^-)] . \tag{8}$$

This can then be solved with boundary condition (2) and the resulting photon and carrier distributions can be used to compute from Eq. (3c) the factors B_i for each mode. The ratio of the photon number in the ith mode to that in the 0th mode is derived from Eq. (3a):

$$\frac{\overline{P}_i}{\overline{P}_0} = \frac{\beta}{\beta + (B_0 - B_i)(1 - N_{om}/\overline{N})\overline{P}_0} . \tag{9}$$

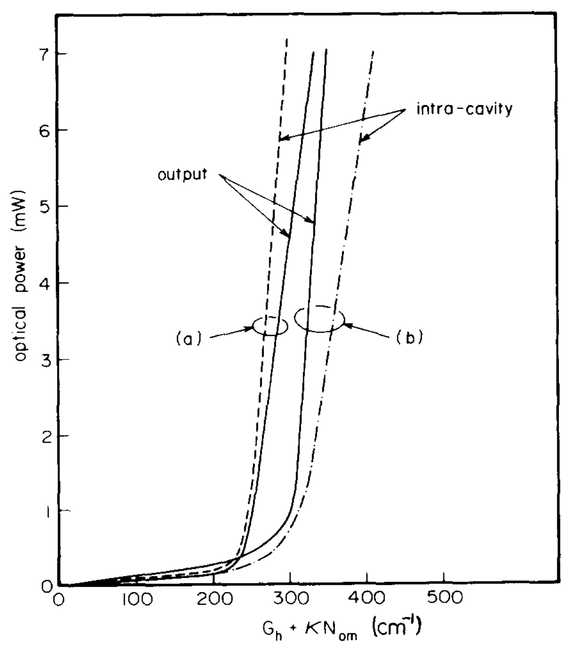

FIG. 1. Output optical power (solid lines) from the exit facet of (a) a common laser with $R_1 = R_2 = 0.3$ and (b) an AR coated laser with $R_1 = 0.01$, $R_2 = 0.3$, plotted as a function of $G_h + \kappa N_{om}$, which is proportional to the pump current.

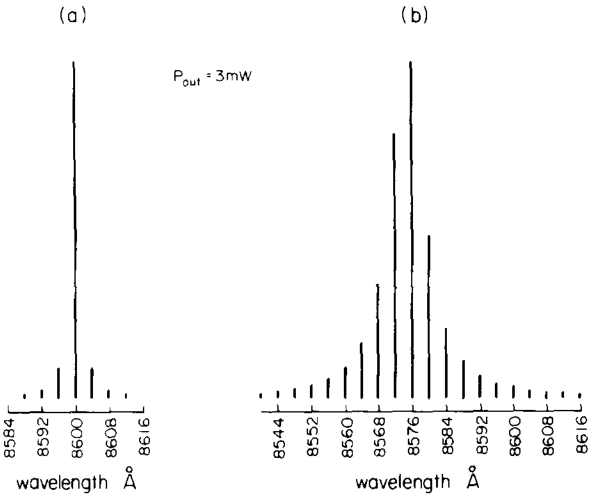

FIG. 2. Lasing spectrum of the two lasers in Fig. 1 at 3-mW output from the exit facet.

Given a pump level (designated by the unsaturated gain G_h), the laser length and facet reflectivities, one can self-consistently compute from Eqs. (7)–(9) the total power ratio S and the power in each mode.

Figure 1 shows the computed optical power output (all modes) from the exit facet as a function of $(G_h + \kappa N_{om})$ (which is proportional to the pump current) for (a) a common laser with $R_1 = R_2 = 0.3$ and (b) an AR coated laser with R_2 reduced to 1%. Also shown is the average intracavity optical power in both cases. At comparable output power levels, the significantly lower internal photon density in the AR coated laser manifests the large number of longitudinal modes, evident from Eq. (9).

Figure 2 shows the principle results of this study: the longitudinal mode spectrum of the two lasers in Fig. 1 is shown at identical output powers of 3-mW/facet. These results are consistent with that observed in Refs. 11 and 12. At higher output power levels (> 7–8 mW/facet) though, both lasers give essentially single-mode output, although the uncoated laser spectrum is somewhat "purer." Lasers with increased facet reflectivity exhibit spectrum of even higher purity, due principally to the higher intracavity optical power and the smaller variation in the gain spectrum along the length of the cavity.

This research was supported by the Defence Advanced Research Project Agency.

[1]H. Statz and G. deMars, *Quantum Electronics*, edited by C. H. Towns (Columbia University, New York, 1960).
[2]L. W. Casperson, J. Appl. Phys. **46**, 5194 (1975).
[3]D. Renner and J. E. Carroll, Electron. Lett. **14**, 781 (1978).
[4]P. Brosson, W. W. Ruble, N. B. Patel, and J. E. Ripper, IEEE J. Quantum Electron. **QE-17**, 714 (1981).
[5]T. Tsukada, J. Appl. Phys. **45**, 4899 (1974).
[6]H. Namizaki, IEEE J. Quantum Electron. **QE-11**, 427 (1975).
[7]K. Aiki, M. Nakamura, T. Kuroda, J. Umeda, R. Ito, and M. Maeda, IEEE J. Quantum Electron. **QE-14**, 89 (1978).
[8]J. Katz, S. Margalit, D. P. Wilt, P. C. Chen, and A. Yariv, Appl. Phys. Lett. **37**, 987 (1980).
[9]M. Yamada and Y. Suematsu, J. Appl. Phys. **52**, 2653 (1981).
[10]K. Seki, T. Kamiya, and H. Yanai, IEEE J. Quantum Electron. **QE-17**, 706 (1981).
[11]R. G. Plumb and J. P. Curtis, Electron Lett. **16**, 706 (1980).
[12]M. Ettenberg, D. Botez, D. B. Gilbert, J. C. Connolly, and H. V. Kowger, IEEE J. Quantum Electron. **QE-17**, 2211 (1981).
[13]H. C. Casey and M. B. Panish, *Heterostructure Lasers* (Academic, New York, 1978), Part A, p. 172.
[14]L. W. Casperson, J. Appl. Phys. **48**, 258 (1977).

Femtosecond interferometry for nonlinear optics

J-M. Halbout and C. L. Tang
Materials Science Center, Cornell University, Ithaca, New York 14853

(Received 11 January 1982; accepted for publication 12 February 1982)

A technique of time-resolved interferometry capable of observing nonlinear optical phenomena down to 70 fs is presented. We report the direct observation of the rotational contributions to the nonlinear refractive index of molecular liquids using this technique. The subpicosecond dynamics of such a nonlinearity in CS_2 are investigated. This technique can be readily extended to solids, in particular laser glasses.

PACS numbers: 42.65. – k, 07.60.Fs

A wide variety of nonlinear optical effects arises from the nonlinear polarization $\mathbf{P}^{(3)}$, third order in the electric field. There are two intrinsic contributions to this third-order nonlinearity. First, the nonlinear distortion of the electronic distribution around a fixed nuclear configuration of the molecules gives rise to the "purely electronic" contribution. The second contribution is of "nuclear" origin, arising from the optical field induced motions of the nuclei of the